Chapter 26

Inundation schemes

26.1 Test case *flood2d*

26.1.1 Description of the problem and model setup

The 2DV test case ***flood2d*** simulates the flooding and drying by an oscillating current inside a straight channel using two different bathymetries, shown in Figures 26.1. The solid line represents the bathymetry, the dotted line the initial water level. The area at the upper level to the right is initially taken as dry. All simulations start at ebb tide. In the first case, the water rises along an upsloping bottom while the second case represents the flooding over a barrier.

The channel, directed in the X-direction, has a length of 6810 m and is discretised using 100 cells in the horizontal and 20 vertical levels. Tidal forcing is imposed by using the local solution method (4.360) and specifying the surface elevation at the western boundary in harmonic form

$$\zeta = \zeta_a \cos(\omega t - \pi) \tag{26.1}$$

where $\zeta_a = 2$ m and $\omega = \pi/6$ rad/h is the semi-diurnal S_2 frequency. The time steps are limited by the 2-D and 3-D CFL stability criteria (5.4) and (5.6). Values are $\Delta\tau = 3$ s and $\Delta t = 15$ s for the first bathymetry. The same 2-D and 3-D time step of 3 s has to be taken for the second bathymetry. At the initial time the water level $\zeta(0)$, outside the dry area (see Figure 26.1), is set to a constant value (-2 m in the first and -3 m in the second case) so that the total water depth is below the reference level used in the definition of the bathymetry.

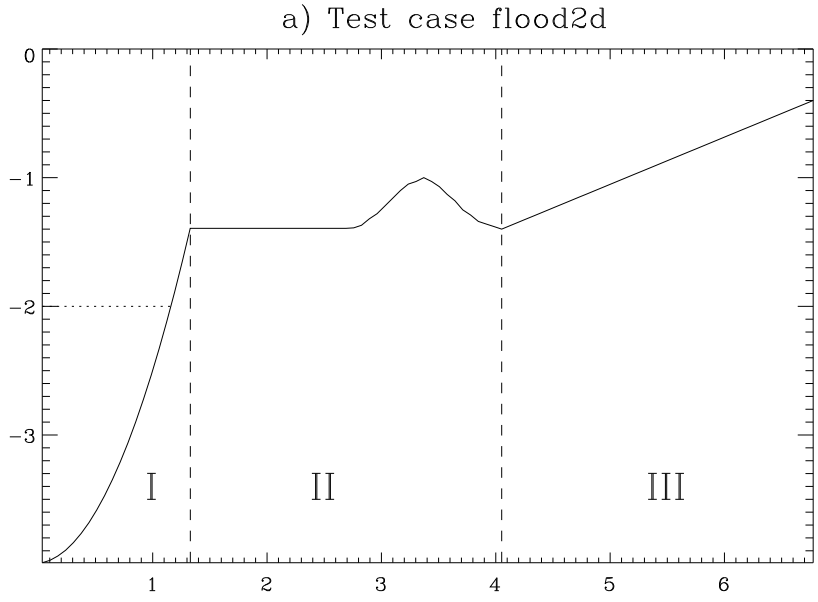

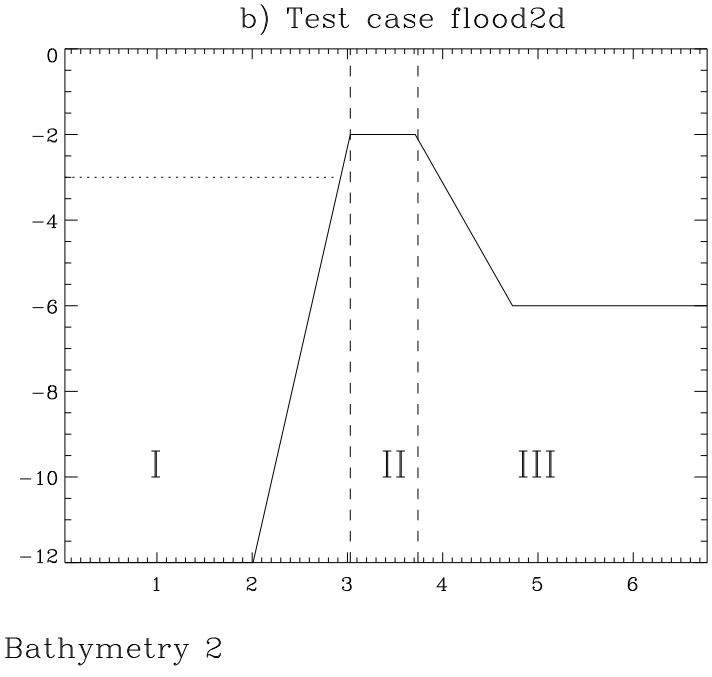

Figure 26.1: Test case ***flood2d***. Bathymetry (solid) and initial water level (dots) for configuration 1 (a) and 2 (b) used in ***flood2d***. Also shown are the three areas used for the definition of test case parameters.

26.1.2 Experiments and output parameters

The following experiments have been defined:

A **:** First bathymetry using the drying/wetting scheme without mask criteria

B **:** First bathymetry using the drying/wetting scheme with the default mask criterium

C **:** Second bathymetry using the drying/wetting scheme without mask criteria

D **:** Second bathymetry using the drying/wetting scheme with the default mask criterium

The simulations are performed for 24 h or two tidal cycles. The flooding and subsequent drying of the land areas during the first tidal cycle are shown in Figures 26.2 and 26.3 for respectively experiments ***B*** and ***D***. Time series of the dry area fraction, and the maximum and mean depth error Δh_e, as defined in Section 5.4.1, are given in Figures 26.4, respectively 26.5.

The following output parameters are defined:

volerr Volume error in %, which results from adding or removing water to the domain, normalised by the total domain volume. In the case of a mass conserving numerical scheme, the change of the total volume $\mathcal{V}$ in time should equal the net amount of water entering or leaving the domain at the open boundaries, which is obtained by integrating the continuity equation over the whole domain

$$\frac{\partial \mathcal{V}}{\partial t} = -\int_{\mathcal{B}} U_n \, dl \tag{26.2}$$

where the integral at the right hand side is taken over the open boundary $\mathcal{B}$ and U_n the outward directed normal component of the transport. If mass is not conserved, the amount of volume $\delta\mathcal{V}$ added or removed from the area satisfies the equation

$$\frac{\partial}{\partial t}\delta\mathcal{V} = \frac{\partial \mathcal{V}}{\partial t} + \int_{\mathcal{B}} U_n \, dl \tag{26.3}$$

For the present setup, the discretised form of (26.3) is given by

$$\delta\mathcal{V}^{m+1} = \delta\mathcal{V}^{m} + \Delta^2 \sum_i (H_{i1}^{m+1} - H_{i1}^{m}) - U_b W \delta\tau \tag{26.4}$$

where Δ is the uniform horizontal grid spacing, W the width of the (western) open boundary and U_b the X-component of the transport at the open boundary. Since $W = \Delta$, the normalised volume error is given by

$$\left(\frac{\delta\mathcal{V}}{\mathcal{V}}\right)^{m+1} = \frac{\delta\mathcal{V}^m}{\mathcal{V}^{m+1}} + \frac{\Delta\sum_i(H_{i1}^{m+1} - H_{i1}^m) - U_b\Delta\tau}{\Delta\sum_i H_{i1}^{m+1}} \qquad (26.5)$$

The parameter volerr is defined as the term on the right hand side of (26.5) multiplied by 100.

depmeanerr Horizontally averaged depth error in cm.

depmaxerr Maximum depth error in cm.

dryarea % of the area which is (temporarily) dry. A cell is considered as dry if the total water depth equals d_{min} (iopt_fld=1) or the cell is inactive (iopt_fld=2).

volume1 % of water volume residing in area I (see Figure 26.1).

volume2 % of water volume residing in area II.

volume3 % of water volume residing in area III.

uvelmax Maximum value of the horizontal current (cm/s).

uvelmin Minimum value of the horizontal current (cm/s).

wphysmax Maximum value of the physical vertical current (mm/s).

wphysmin Minimum value of the physical vertical current (mm/s).

26.1.3 Results

- Comparison of the test case parameters and time series of the currents and elevations (not shown for tests ***A*** and ***C***) reveal that the differences between the two drying/wetting algorithms are small. Only noticeable difference is that the dry area is slightly larger for the second scheme. The main difference is mass conservation, further discussed below.

- In the sloping bottom experiment, the flow of the rising water retards when the water mass reaches the edge of the shelf at 1.4 m depth. Flow divergence, followed by convergence, is observed when the tidal wave moves over the shallower area in the middle of the channel. This shallowing effect is reduced with the approach of the flood tide. The reverse effect occurs when the water recedes from the coast. As the water depth over the outer shelf approaches its minimal value, the flow retards by bottom friction. This explains why water is still falling from

the edge into the deeper basin at the ebb tide even when the water level in the deeper part is already 0.6 m below the shelf.

- The second experiment with the large obstacle in the middle of the channel, is a similar, but more extreme case. As the water mass moves past the obstacle, the water forms a thin layer and falls abruptly into the coastal basin (Figure 26.3a). The wave, generated by the falling water masses downhill of the slope, reflects at the coast[1]. The reflected wave opposes the tidal current (Figure 26.3b) and even creates a temporarily flow reserval. At the approach of the maximum flood, the wave decreases in amplitude and the tidal current reappears (Figure 26.3c). Some similar wave behaviour is observed at ebb tide when the layer above the obstacle thins and water falls downhill into the western deeper part of the channel. The wave does not propagate entirely through the open boundary which could explain the vertical oscillations at ebb tide (Figure 26.3f). The oscillation gradually damps out at the start of the next tidal cycle and disappears about one hour after the onset of the flood tide (not shown).

- Mass conservation can be verified by checking the values of the parameters depmaxerr, depmeanerr and volerr in the *.tst* files and from Figure 26.5. As explained in Section 5.4.1, virtual water is added to the water column when the water depth drops below h_{min} which occurs during the drying (ebb) phase of the tidal cycle.

  - The results, in case of the first configuration, are now manifestly different for the two schemes. For the first one (without mask function) the maximum error, occurring close to the coast, increases by more than 1 cm at each cycle and the volume error at the end of the simulation becomes 0.4%. Using the second scheme (with mask function) these values become 0.008 cm and 0.005%, which may be considered at or below noise level.
  - For the second configuration, drying only occurs when the water shallows above the obstacle. Values for the maximum depth and volume error remain sufficiently small for both schemes, implying that mass is reasonable well conserved.

[1]It is remarked that the hydrostatic assumption may no longer be valid in this case.

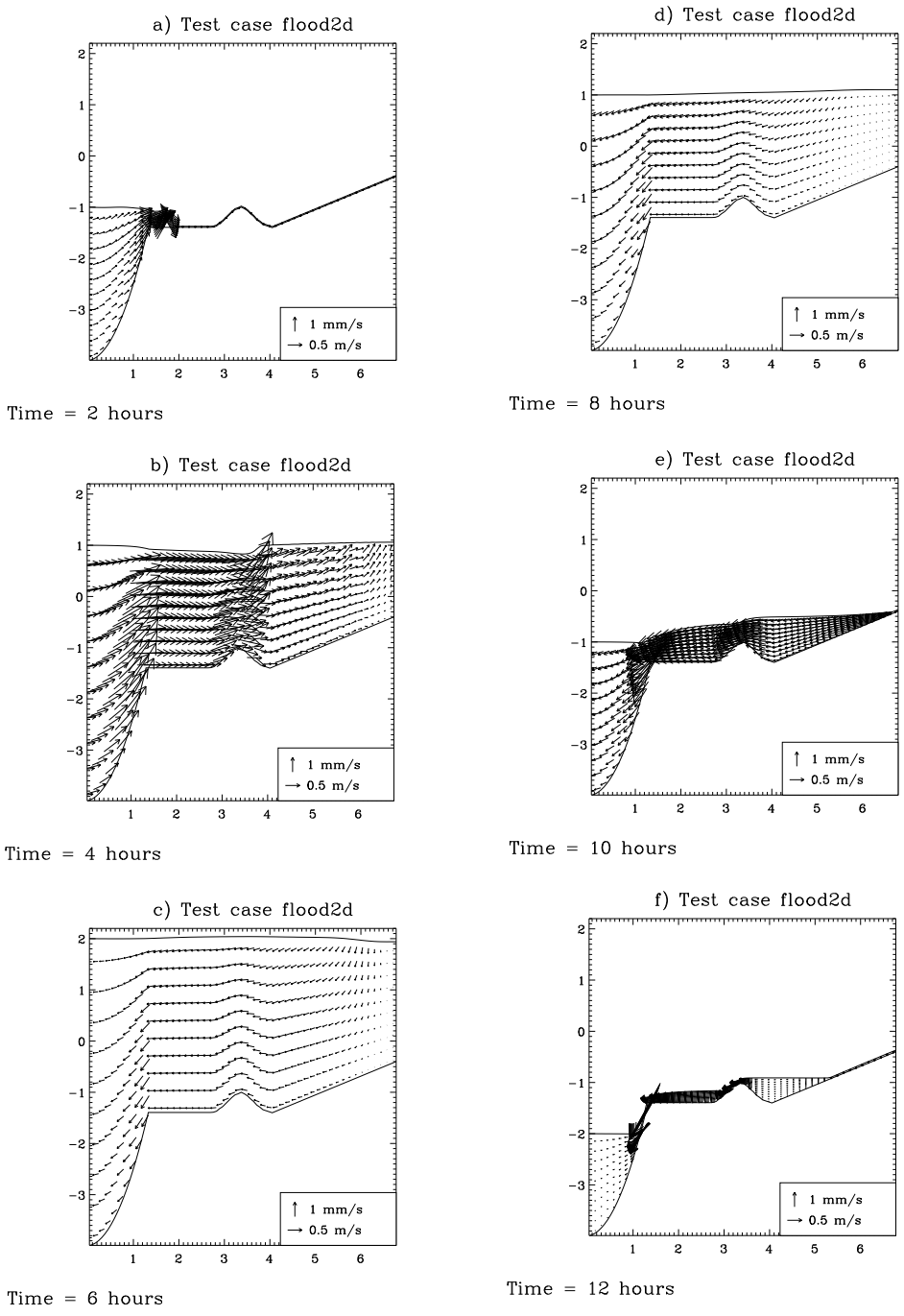

Figure 26.2: Test case ***flood2d***. Time series of currents and surface elevations during the first tidal cycle and experiment ***flood2dB***.

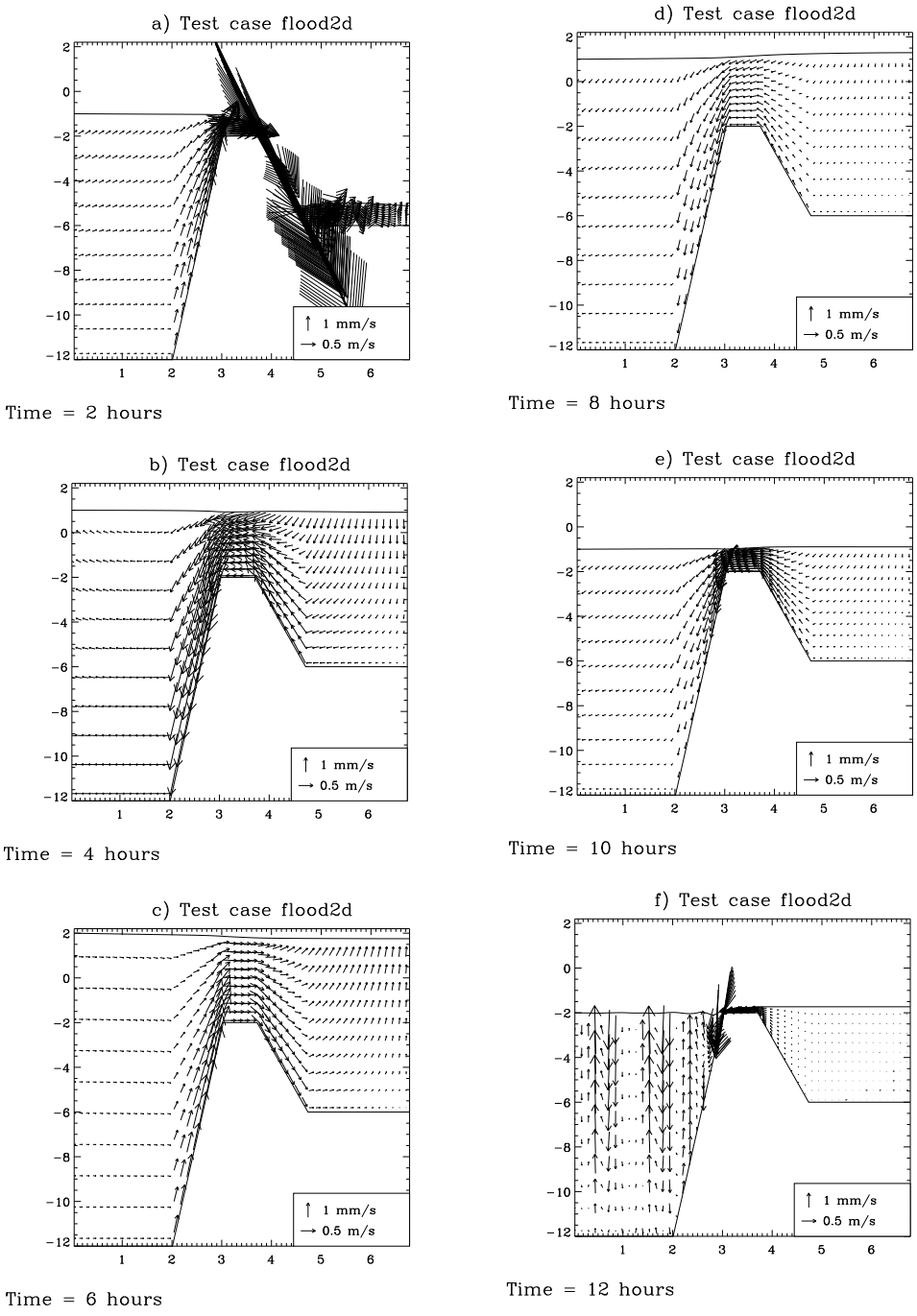

Figure 26.3: Test case ***flood2d***. Time series of currents and surface elevations during the first tidal cycle and experiment ***flood2dD***.

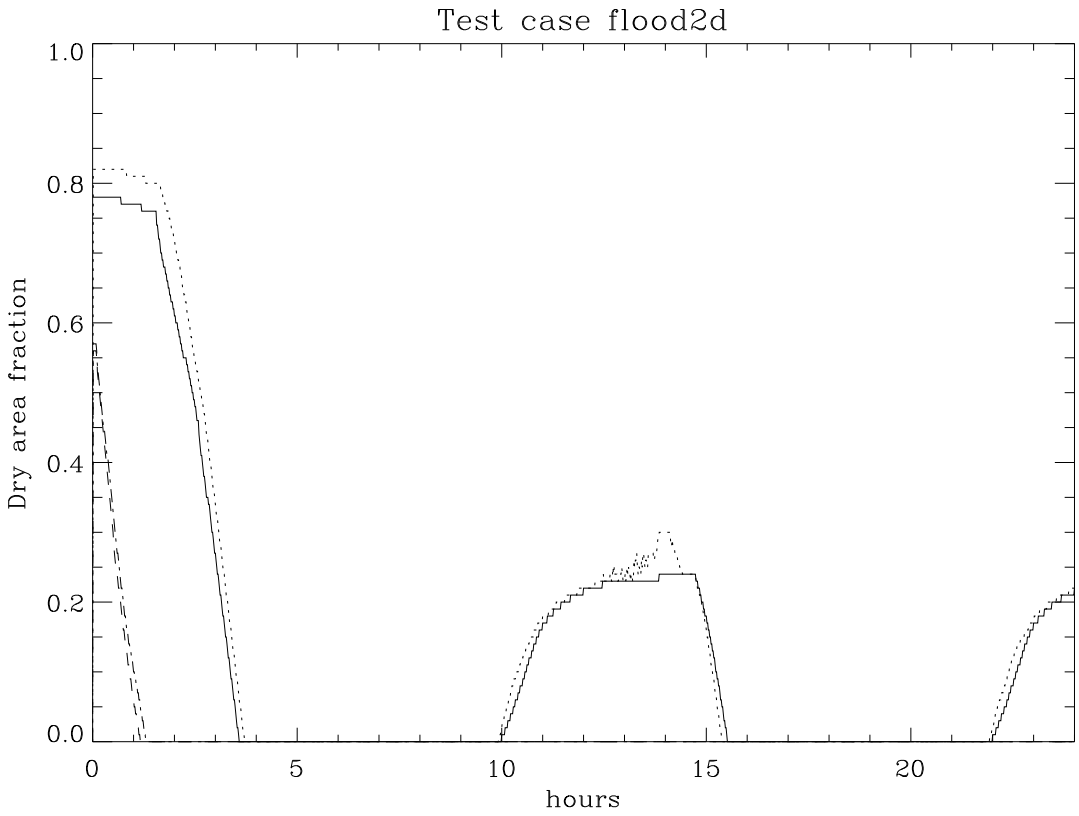

Figure 26.4: Test case ***flood2d***. Time series of the dry area fraction and experiment ***A*** (solid), ***B*** (dots), ***C*** (dashes) and ***D*** (dash-dots).

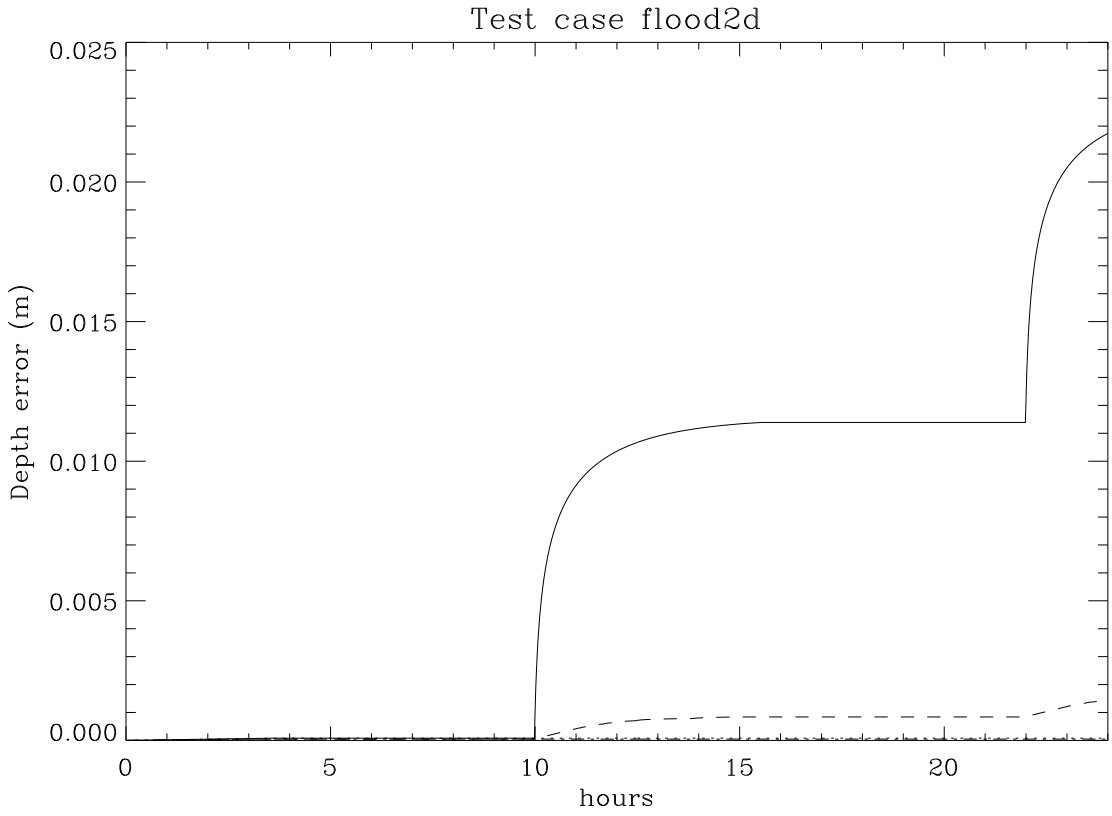

Figure 26.5: Test case ***flood2d***. Time series of the maximum water depth error for experiment ***A*** (solid), ***B*** (dots), and the mean depth error for experiment ***A*** (dashes) and ***B*** (dash-dots).

26.2 Test case *flood3d*

26.2.1 Description of the problem and model setup

Test case ***flood3d*** consists of a series of experiments simulating flooding and drying by an oscillating tidal current in a rectangular basin. The experiments are conducted for three different bathymetries shown in Figure 26.6.

The basin has a size of 6810 m. The model grid uses 100 cells in each horizontal direction and 20 vertical levels. A tidal current enters the basin through the western boundary. All other lateral boundaries are closed. The tide is imposed by using the local solution method (4.360) and specifying the surface elevation at the western boundary using the harmonic form (26.1) with $\zeta_a = 2$ m and the semi-diurnal S_2 frequency.

The time step is $\Delta\tau = 3$ s for the 2-D mode. The 3-D time step is respectively 30, 15 and 3 s for respectively the first, second and third bathymetry. At the initial time the water level $\zeta(0)$, outside the inital dry area (see Figure 26.6), is set to a constant value -2 m so that total water depth is below the reference level used in the definition the bathymetry.

26.2.2 Experiments and output parameters

The following experiments have been defined:

A **:** Flow over a temporarily inundated mountain in the center of the domain (first bathymetry).

B **:** Flow over a gently sloped "crater" rim in the center of the domain (second bathymetry).

C **:** Flow over a strongly sloped "crater" rim (third bathymetry).

D **:** As experiment ***C*** now using a 2-D (depth-averaged) grid.

All experiment use the same drying/wetting scheme with the default mask function.

Time series of currents and water levels for the first tidal cycle are shown in Figures 26.7, 26.9, 26.11 for respectively experiments ***A,B,C***. Depth mean currents and total water depths are displayed as time series for the first cycle in Figures 26.8, 26.10, 26.12, 26.13 for respectively experiments ***A, B, C, D***. Time series of the dry area fraction, and the maximum depth error Δh_e, as defined in Section 5.4.1, are given in Figures 26.14, respectively 26.15.

The following output parameters are defined:

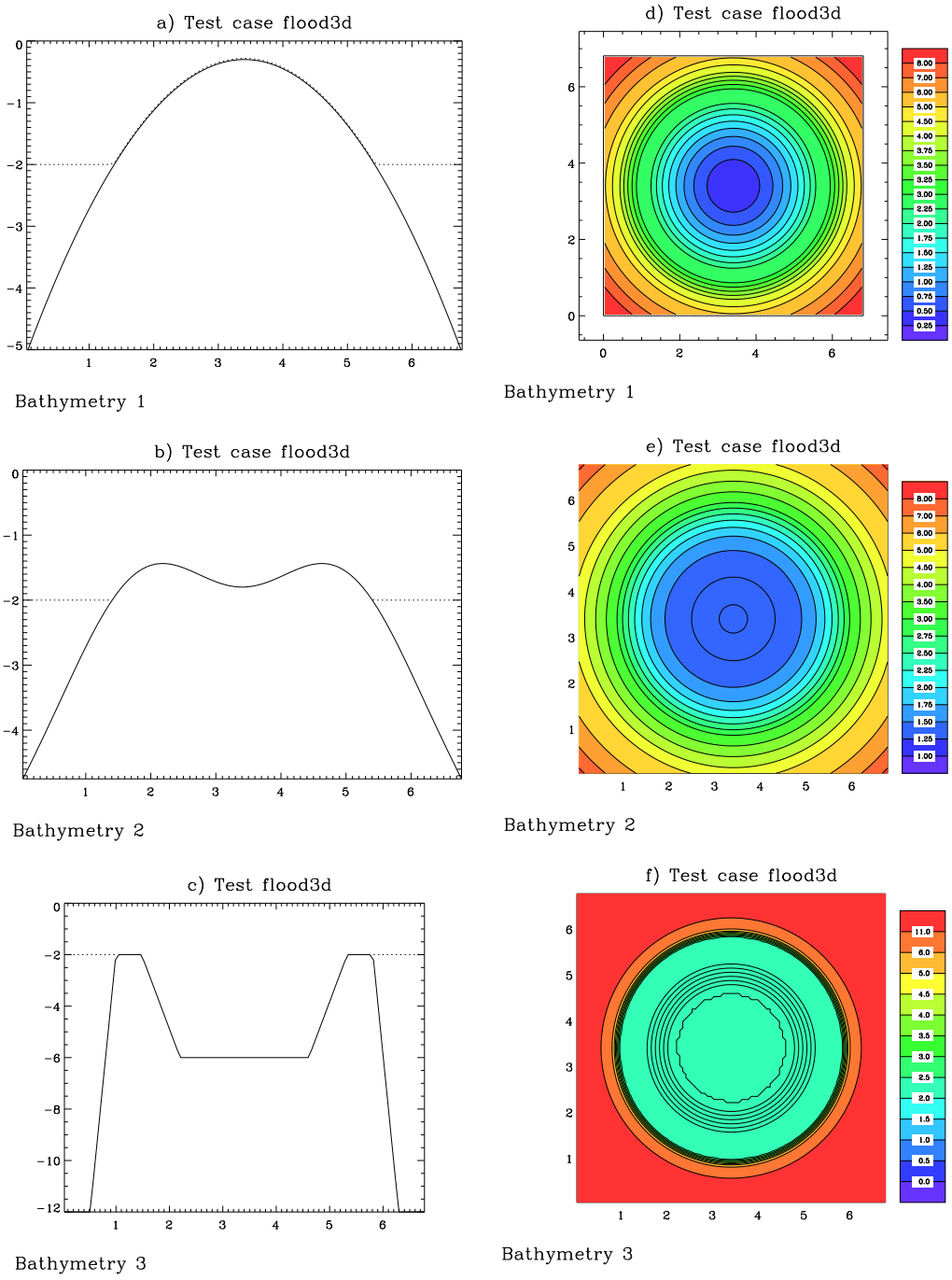

Figure 26.6: Test case ***flood3d***. Bathymetry (solid) and initial water level (dots) along a transect normal to the open boundary and through the center of the basin for the three different configurations used in ***flood3d*** (left). Top view of the bathymetry (right).

volerr Volume error in %,which results from adding or removing water to the domain, normalised by the total domain volume. In analogy with (26.5) this is given by

$$\left(\frac{\delta\mathcal{V}}{\mathcal{V}}\right)^{n+1} = \frac{\delta\mathcal{V}^n}{\mathcal{V}^{n+1}} + \frac{\Delta^2 \sum_{i,j}(H_{ij}^{n+1} - H_{ij}^n) - WU_b\Delta\tau}{\Delta^2 \sum_{ij} H_{ij}^{n+1}} \quad (26.6)$$

multiplied by a factor 100.

depmeanerr Horizontally averaged depth error in cm.

depmaxerr Maximum depth error in cm.

dryarea % of the area which is (temporarily) dry (inactive).

ekin Volume integrated kinetic energy (10^9J).

epot Volume integrated potential energy (10^9J).

etot Volume integrated total energy (10^9J).

edissip Domain integrated (negative) energy dissipation (10^4W).

uvelmax Maximum value of the u-current (cm/s).

uvelmin Minimum value of the u-current (cm/s).

vvelmax Maximum value of the v-current (cm/s).

vvelmin Minimum value of the v-current (cm/s).

wphysmax Maximum value of the physical vertical current (mm/s).

wphysmin Minimum value of the physical vertical current (mm/s).

26.2.3 Results

- It is readily observed that all solutions are symmetric with respect to the vertical transect in the X-direction passing through the center of the basin.

- In the case of an isolated hill (experiment ***A***), the flooding and drying process proceeds smoothly. During the rising tide, the incoming eastward flow in the central part deflects in the along-hill direction when it approaches the hill boundary. In the more southern (northern) parts the water flows unimpeded until it reaches the solid eastern boundary where it deflects to the left (right). The result is a cyclonic (anticyclonic) circulation below (above) the center line during the rising tide. The circulation reverses with the onset of the ebb tide. At first, the top of the hill is still inundated and the flow is mainly westward. As soon as the drying starts on the top of the hill, the water masses close to the dry area start to flow both along and away from the hill.

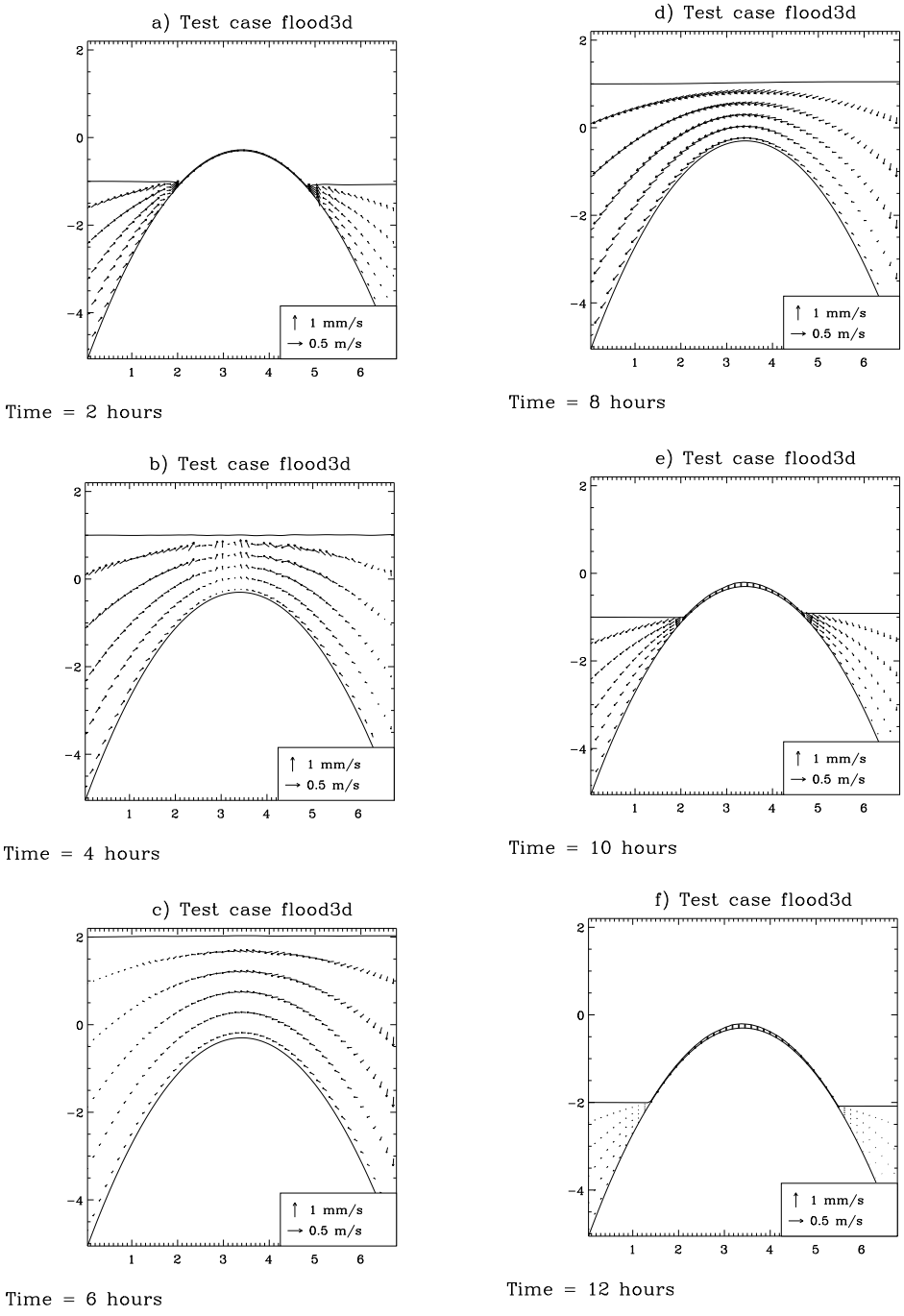

Figure 26.7: Test case ***flood3d***. Time series of currents and elevations during the first tidal cycle and along a transect normal to the open boundary and through the center of the basin for experiment ***flood3dA***.

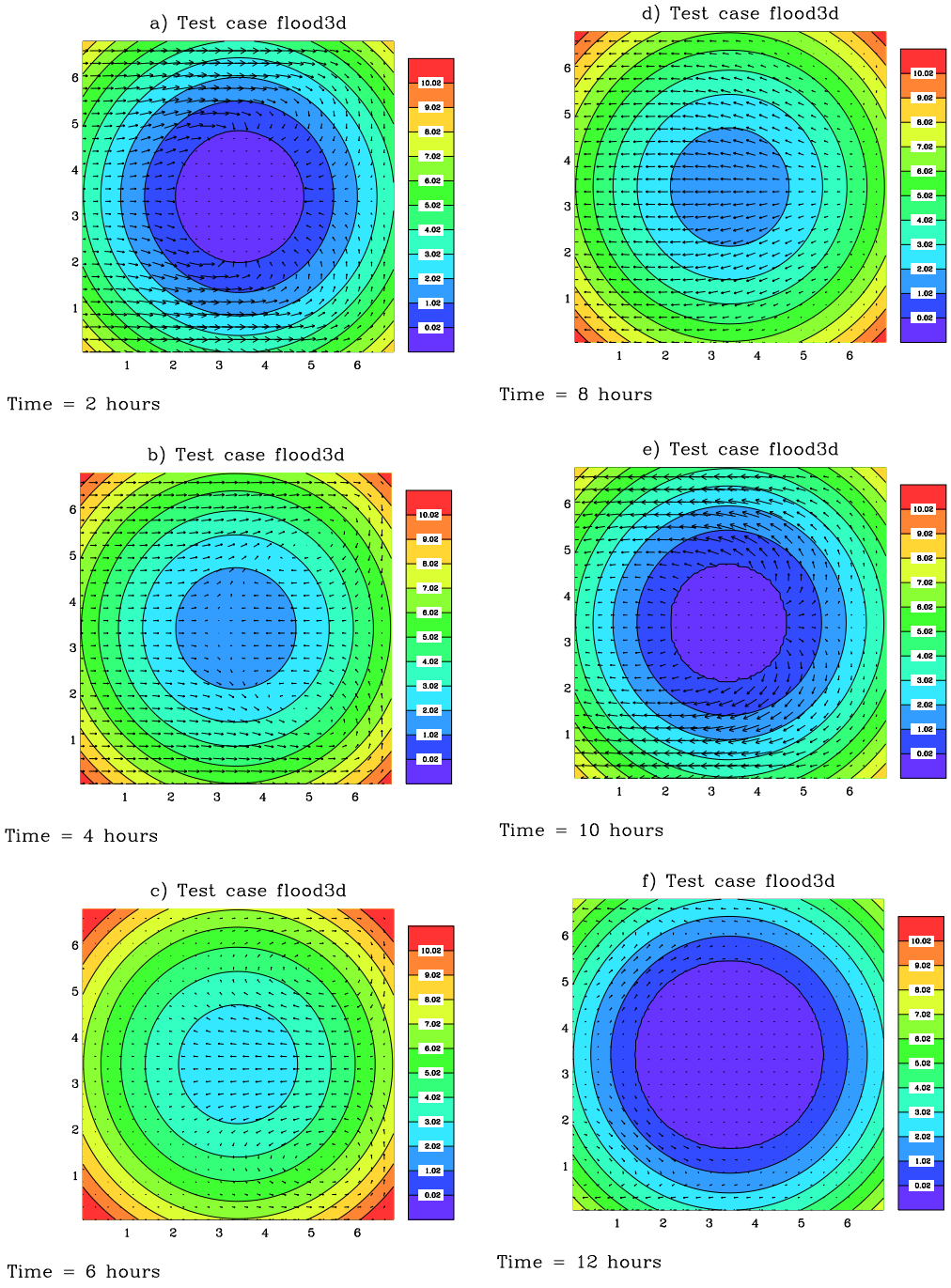

Figure 26.8: Test case ***flood3d***. Time series of horizontal depth mean currents and water depths during the first tidal cycle and experiment ***flood3dA***.

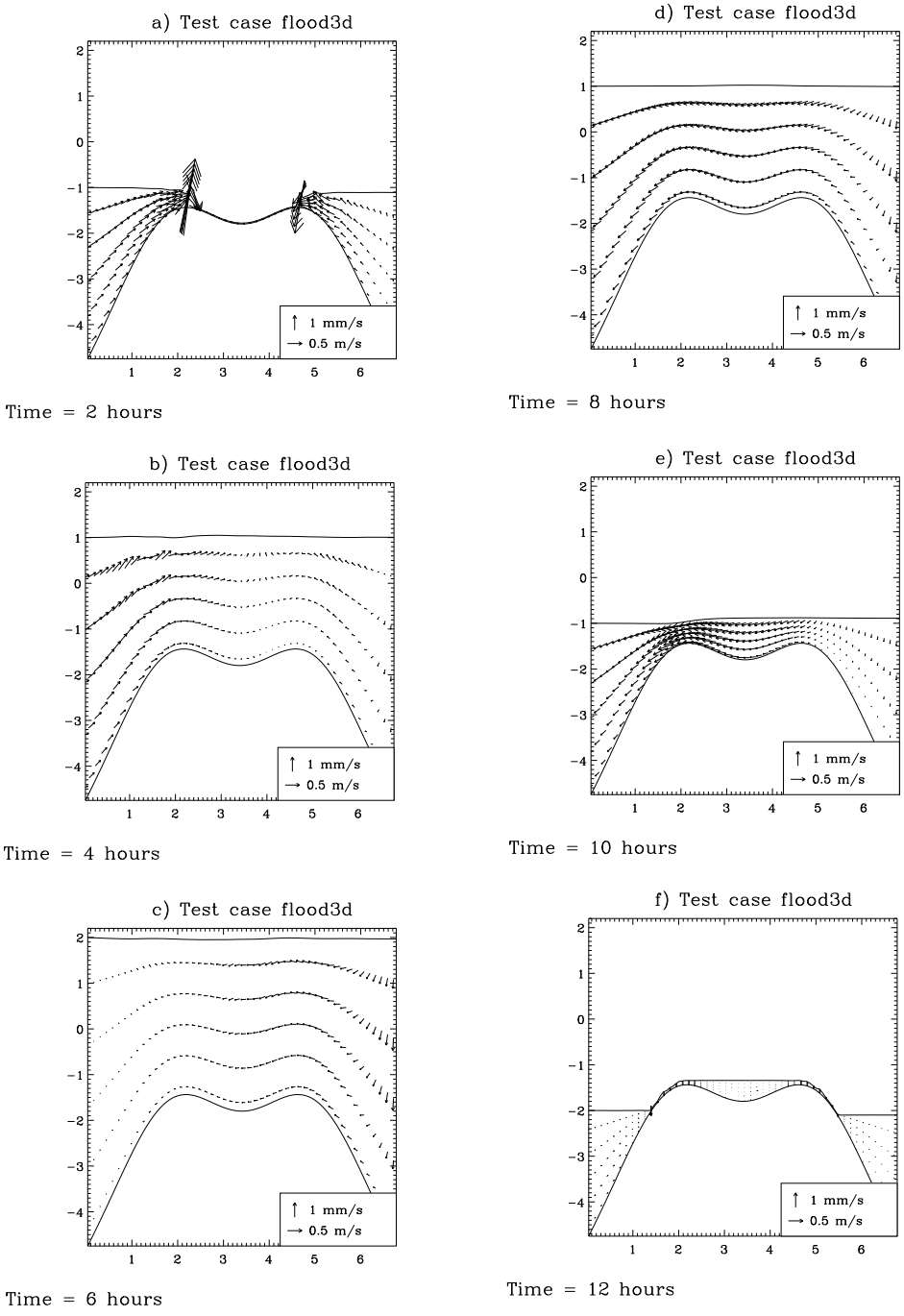

Figure 26.9: Test case ***flood3d***. Time series of currents and elevations during the first tidal cycle and along a transect normal to the open boundary and through the center of the basin for experiment ***flood3dB***.

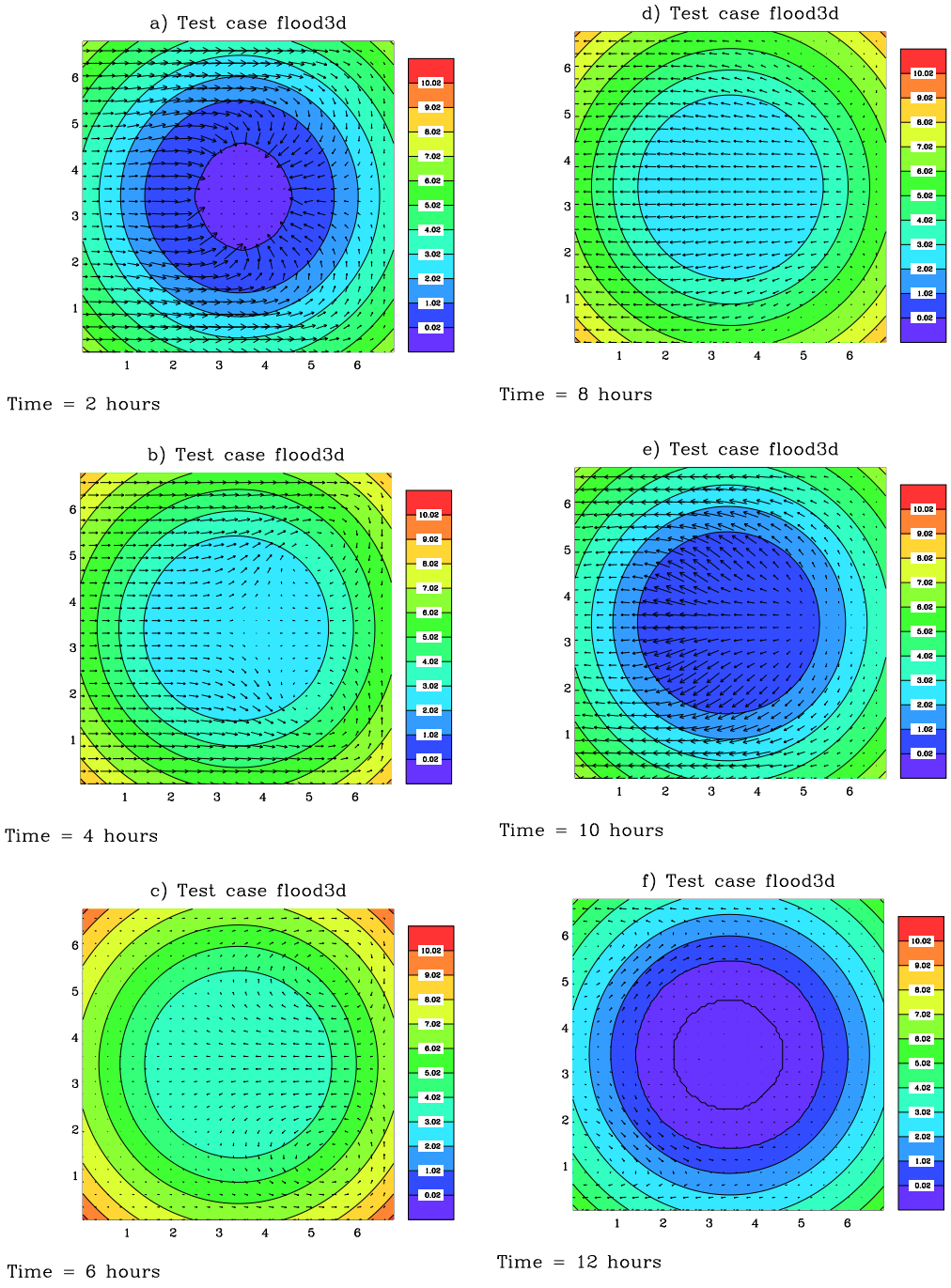

Figure 26.10: Test case ***flood3d***. Time series of horizontal depth mean currents and water depths during the first tidal cycle and experiment ***flood3dB***.

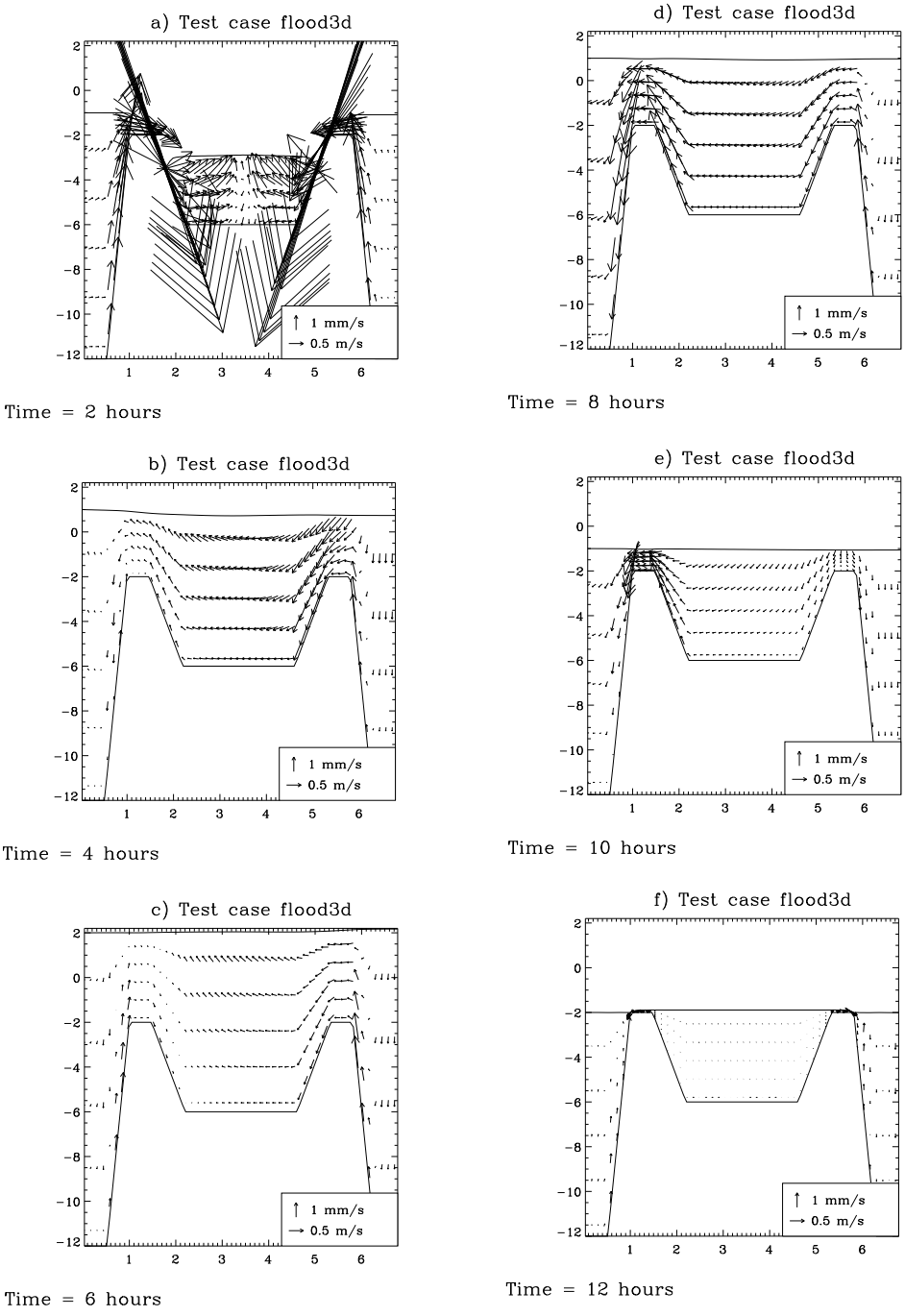

Figure 26.11: Test case ***flood3d***. Time series of currents and elevations during the first tidal cycle and along a transect normal to the open boundary and through the center of the basin for experiment ***flood3dC***.

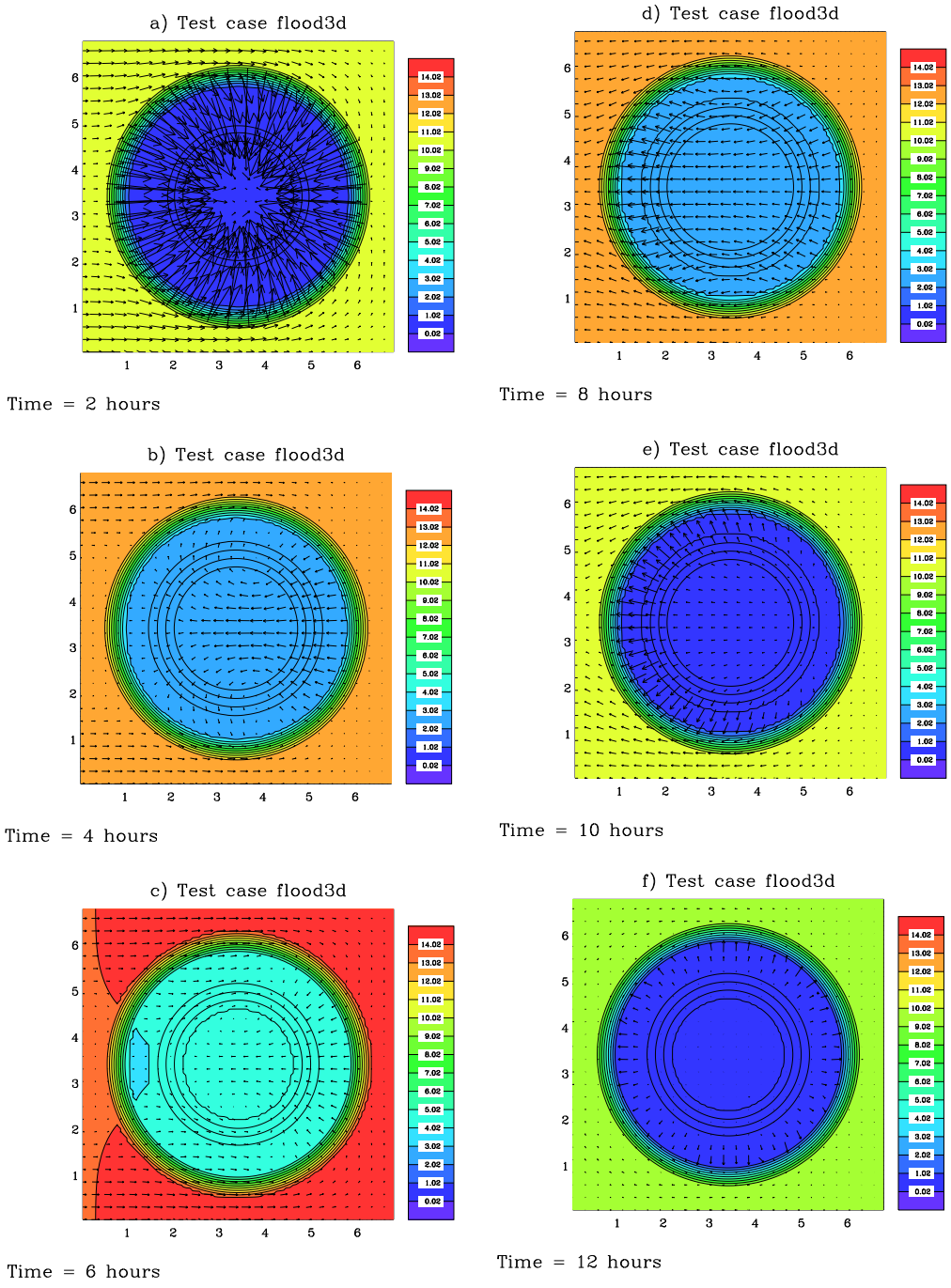

Figure 26.12: Test case ***flood3d***. Time series of horizontal depth mean currents and water depths during the first tidal cycle and experiment ***flood3dC***.

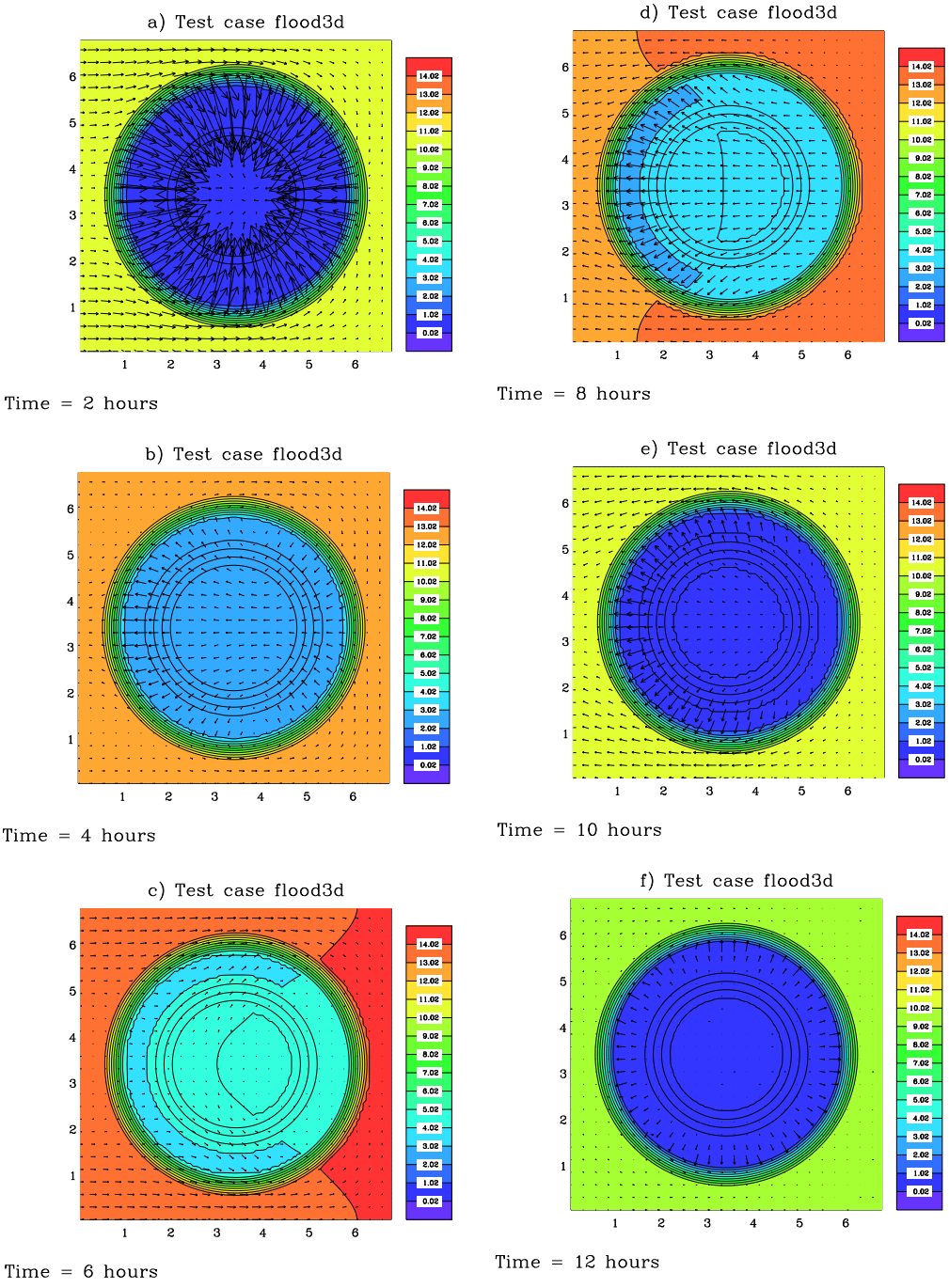

Figure 26.13: Test case ***flood3d***. Time series of horizontal depth mean currents and water depths during the first tidal cycle and experiment ***flood3dD***.

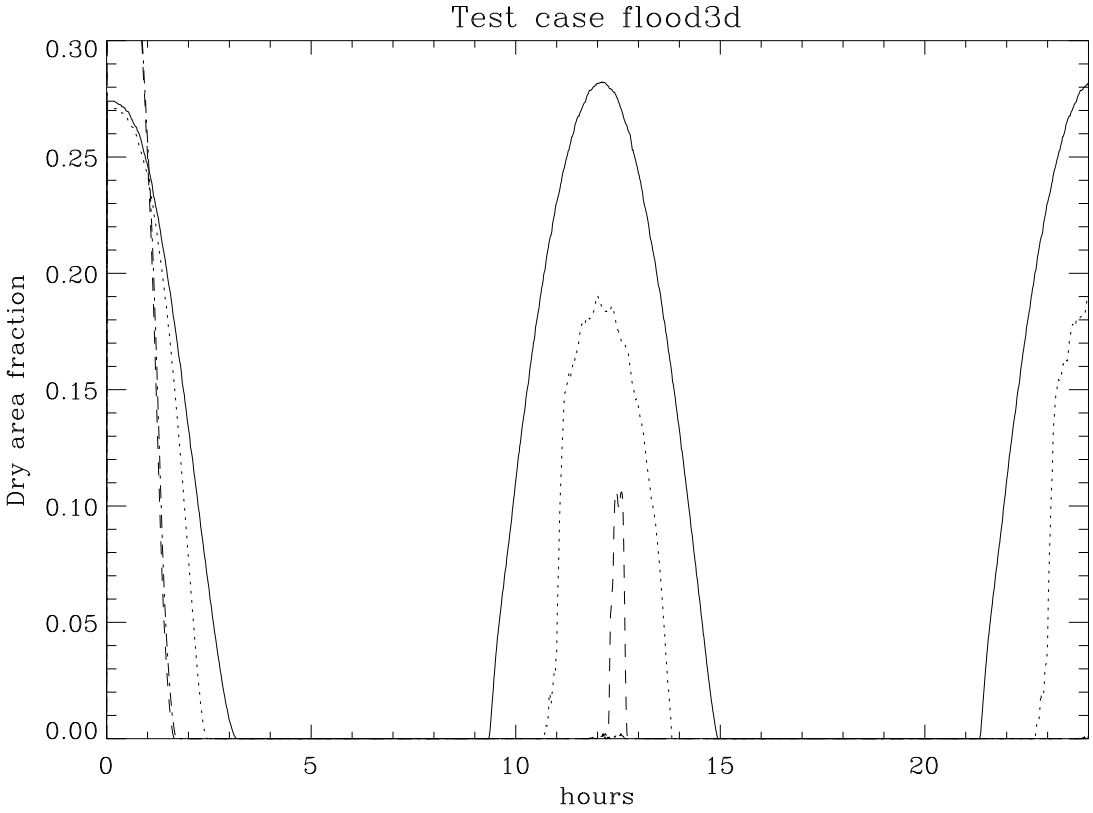

Figure 26.14: Test case ***flood3d***. Time series of the dry area fraction and experiment ***A*** (solid), ***B*** (dots), ***C*** (dashes) and ***D*** (dash-dots).

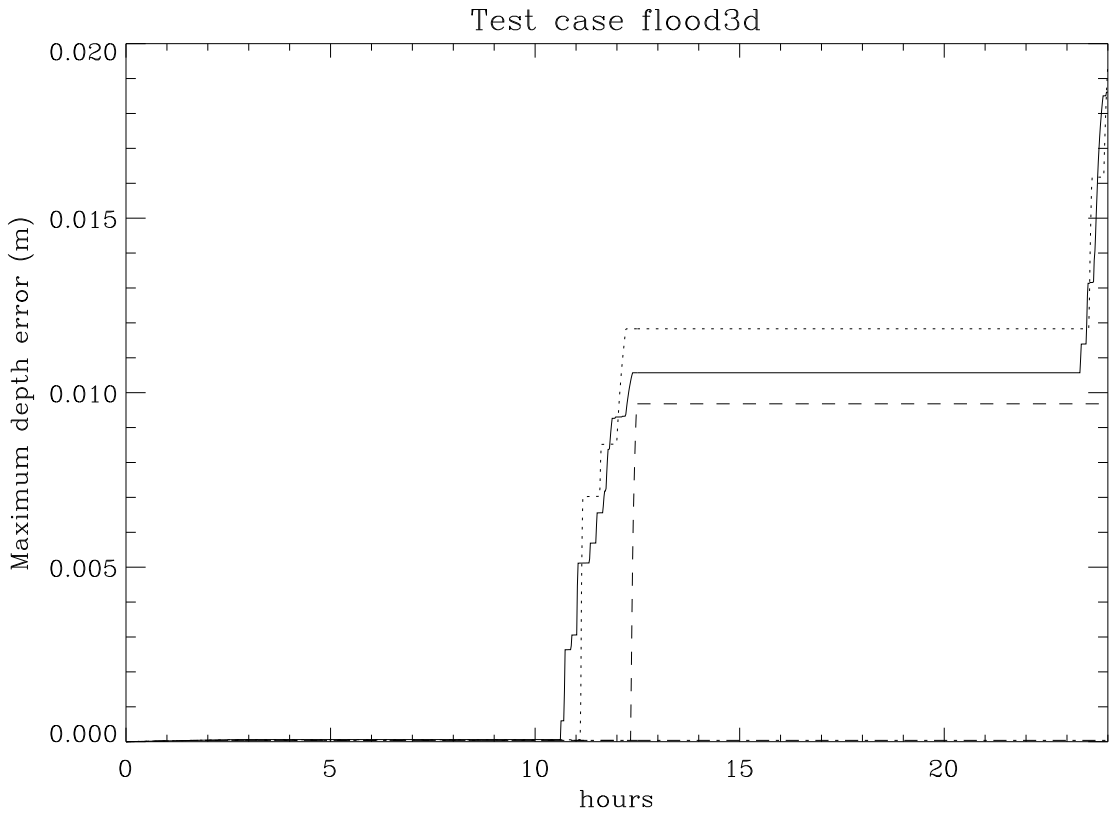

Figure 26.15: Test case ***flood3d***. Time series of the maximum water depth error for experiment ***A*** (solid), ***B*** (dots), ***C*** (dashes) and ***D*** (dash-dots).

- Experiment ***B*** is similar to the previous one, until the water reaches the rim of the crater, when the flow retards upslope and accelerates downslope towards the center of the (inner) basin. Comparison of Figures 26.8 and Figures 26.10 shows that the general circulation patterns are similar for ***A*** and ***B***.

- The bathymetry of experiment ***C*** is similar to the previous one, except that the slopes on the outer and inner side of the crater are much steeper in the latter case. When the water flows over the rim in experiment ***C***, it falls rapidly towards the center[2]. Contrary to the analogous 2DV case test case ***flood2dD***, the water comes from all directions. The infall is, moreover, not radially symmetric. Once the infalling water reaches the center, an outgoing non-symmetric radial wave is created, opposing the masses still falling in the crater, The result, as seen in Figure 26.11b, is that water starts to move out along the western rim and to move in with higher speed from the eastern side. The rim currents slow down at the approach of high tide and the flow at the western side becomes inwards again. The drying process during the ebb proceeds in a much smoother way, since the crater is already filled with water.

- Although test ***D*** uses the same bathymetry as experiment ***C***, the results at high water, observed in Figures 26.13, are manifestly different. The reason is that the momentum equations are solved without taking account of velocity shear in the former case and it is evident from Figures 26.12 that vertical shear cannot be neglected when water flows over the rim.

- The maximum depth error, which occurs at the top of the mountain (experiment ***A***) or at the crater rim (***B, C***), is of the order of 1 cm per cycle. Note that error in case of the 2-D test ***D*** is negligible small, which may be related to the observation in Figure 26.14 that no "effective drying" (as defined by the mask criterium) seems to occur.

[2]It is remarked that the hydrostatic assumption may no longer be valid in this case.